the frost bacterium *Pseudomonas syringae*. Its ice-nucleating ability arises from proteins bearing a sixfold repetition of octapeptide building blocks. As pointed out by Green and Warren (*4*) and Mizuno (*32*), one may construct molecular models with these octapeptides with lattice (but not structure) symmetry to match the hexagonal lattice of ice. In line with the theme of this report, we propose that the helix dipole moment of the octapeptide moiety may play a role for induced freezing in the pockets between helices of polar arrangement.

REFERENCES AND NOTES

1. K. B. Storey and J. M. Storey, *Sci. Am.* **263**, 62 (December 1990).
2. A. L. DeVries, *Philos. Trans. R. Soc. London Ser. B* **304**, 575 (1984).
3. R. E. Feeney, T. S. Burcham, Y. Yeh, *Annu. Rev. Biophys. Biophys. Chem.* **15**, 59 (1986).
4. R. L. Green and G. J. Warren, *Nature* **317**, 645 (1985).
5. S. E. Lindow, *Annu. Rev. Phytopathol.* **21**, 363 (1983).
6. B. Vonnegut, *J. Appl. Phys.* **18**, 593 (1947).
7. M. L. Corrin and J. A. Nelson, *J. Phys. Chem.* **72**, 643 (1968).
8. D. N. Blair, B. L. Davis, A. S. Dennis, *J. Appl. Meteorol.* **12**, 1012 (1973).
9. B. L. David, L. R. Johnson, F. John Moeng, *ibid.* **14**, 891 (1975).
10. M. Gavish, R. Popovitz-Biro, M. Lahav, L. Leiserowitz, *Science* **250**, 973 (1990).
11. D. Jacquemain *et al.*, *J. Am. Chem. Soc.* **113**, 7684 (1991).
12. J.-L. Wang *et al.*, unpublished results.
13. B. A. Power and R. F. Power, *Nature* **194**, 1170 (1962).
14. N. Barthakur and J. Maybank, *ibid.* **200**, 866 (1963).
15. F. P. Parungo and J. P. Lodge, Jr., *J. Atmos. Sci.* **22**, 309 (1965); *ibid.* **24**, 274 (1967).
16. K. Torii and Y. Iitaka, *Acta Crystallogr. Sect. B* **26**, 1317 (1970); M. Mallikarjunan and S. Thyagaraja Rao, *ibid.* **25**, 296 (1969); M. Coll, X. Solans, M. Font-Altaba, J. A. Subirana, *Acta Crystallogr. Sect. C* **42**, 599 (1986); B. di Blasio, C. Pedone, A. Sirigu, *Acta Crystallogr. Sect. B* **31**, 601 (1975), K. Torii and Y. Iitaka, *ibid.* **27**, 2237 (1971); E. Benedetti, C. Pedone, A. Sirigu, *ibid.* **29**, 730 (1973); K. Torii and Y. Iitaka, *ibid.*, p. 2799; A. McL. Mathieson, *Acta Crystallogr.* **5**, 332 (1952); *ibid.* **6**, 399 (1953).
17. I. Weissbuch, F. Frolow, L. Addadi, M. Lahav, L. Leiserowitz, *J. Am. Chem. Soc.* **112**, 7718 (1990).
18. S. Grayer Wolf, theses, Feinberg Graduate School, Weizmann Institute of Science, Rehovot, Israel (1986 and 1990). In crystal structures of chiral-resolved Val, Leu, Ile, and Met, each hydrogen-bonded layer contains two crystallographically independent molecules related by pseudo-translation in a pseudo-centered cell; the actual space group is $P2_1$. The neighboring layers, related by twofold screw symmetry, are interlinked by N–H···O bonds to form a bilayer. The two independent molecules of neighboring layers forming the bilayer are related by pseudo-twofold symmetry to form a hydrogen-bonded pair. In the crystal structures of Norleu and α-amino octanoic acid, the space group is *C*2, so that the cell is truly centered and the molecules forming a hydrogen-bonded pair are related by twofold symmetry.
19. Hexagonal ice has space group $P6_3/mmc$, with cell dimensions $a = b = 4.5$ Å, $c = 7.3$ Å, $\gamma = 120°$; these dimensions are similar to those of β-AgI with space group $P6_3mc$, cell dimensions $a = b = 4.59$ Å, $c = 7.51$ Å, $\gamma = 120°$, but different from those of the α-amino acids. Cell dimensions of some α-amino acids are as follows: D,L-Val, $a = 5.21$ Å, $b = 22.10$ Å, $c = 5.41$ Å, $\beta = 109.2°$; L-Val, $a = 9.71$ Å, $b = 5.27$ Å, $c = 12.06$ Å, $\beta = 90.8°$; D,L-Leu, $a = 14.12$ Å, $b = 5.39$ Å, $c = 5.19$ Å, $\alpha = 111.1°$, $\beta = 97.0°$, $\gamma = 86.4°$; L-Leu, $a = 9.61$ Å, $b = 5.31$ Å, $c = 14.72$ Å, $\beta = 93.8°$; D,L-Met, $a = 9.89$ Å, $b = 4.70$ Å, $c = 16.74$ Å, $\beta = 102.3°$; L-Met, $a = 9.50$ Å, $b = 5.19$ Å, $c = 15.32$ Å, $\beta = 97.7°$.
20. Because the (0001) face of hexagonal ice is a dominant face, it is reasonable that crystals with such morphology would emerge from the fissure even in the absence of the electric field, as was found for the racemic crystals of Table 1A.
21. J. Donohue, *J. Am. Chem. Soc.* **72**, 949 (1950).
22. H. J. Simpson, Jr., and R. E. Marsh, *Acta. Crystallogr.* **20**, 550 (1966).
23. This property is easily understood in terms of the corresponding 222 point group; a vector (or dipole moment) operated on by the three perpendicular twofold rotation axes of the 222 group has a null resultant value. Thus we have a paradoxical situation such that, although $P2_12_12_1$ is a polar space group in which only the principal planes are nonpolar, the crystal has no net dipole moment.
24. Crystals of L-Ala grown from an aqueous solution did not develop [001] needles with dominant {120} faces, but rather {011}.
25. A. Mostad and C. Romming, *Acta Chem. Scand.* **27**, 401 (1973).
26. A. Mostad, H. M. Nissen, C. Romming, *ibid.* **26**, 3819 (1972).
27. The cell dimensions of these amino acids are as follows: L-Ala, $a = 12.26$ Å, $b = 5.93$ Å, $c = 5.79$ Å, D,L-Ala, $a = 12.04$ Å, $b = 6.04$ Å, $c = 5.81$ Å; L-Tyr, $a = 21.11$ Å, $b = 6.91$ Å, $c = 5.82$ Å; D,L-Tyr, $a = 20.81$ Å, $b = 6.81$ Å, $c = 5.90$ Å.
28. We performed atom-atom potential energy calculations using van der Waals' parameters taken from the 6-9 set of A. T. Hagler, E. Huler, and S. Lifson [*J. Am. Chem. Soc.* **96**, 5319 (1974)] and S. Lifson, A. T. Hagler, and P. Dauber [*ibid.* **101**, 5111 (1979)]. The atomic electrostatic moments, that is, atomic charges, dipoles, and quadrupoles, were derived from the experimental deformation electron density of L-Ala, based on the low-temperature (20 K) x-ray diffraction data of R. Destro, R. E. Marsh, and R. Bianchi [*J. Phys. Chem.* **92**, 966 (1988)] and on that of water in the low-temperature (~100 K) structure of cytosine monohydrate [M. Eisenstein, *Acta Crystallogr. Sect. B* **44**, 412 (1988)]. We obtained the deformation electron densities for both structures using the method of F. Hirshfeld [*Acta Crystallogr. Sect. B* **27**, 769 (1971); *Isr. J. Chem.* **16**, 226 (1977)] and partitioned them to yield the atomic moments according to the stockholder recipe of F. L. Hirshfeld [*Theor. Chim. Acta* **44**, 129 (1977)]. The net charges on the carboxylate CO_2^- and amino NH_3^+ groups of Ala were found to be about 0.6 electron unit.
29. The average calculated interaction energy per water molecule within the single ice-like (0001) bilayer was −3.8 kcal/mol for D,L-Ala and −2.9 kcal/mol for L-Ala; the corresponding values for the double layer were −4.0 and −2.7 kcal/mol, respectively. The interaction is favorable in both cases, but more so for the D,L form, in agreement with experiment.
30. The entropy difference between ice proton-ordered along the hexagonal axis and completely proton-disordered ice in terms of energy is about 0.1 kcal/mol at 0°C.
31. S.-B. Zhu and G. W. Robinson, *J. Chem. Phys.* **94**, 1403 (1991).
32. H. Mizuno, *Proteins* **5**, 47 (1989).

33. This work was supported by the Minerva Foundation, the U S.–Israel Binational Foundation, and the Petroleum Research Fund of the American Chemical Society. M.G. was the recipient of a postdoctoral fellowship from the Feinberg Graduate School of the Weizmann Institute of Science. Dedicated in memory of F L. Hirshfeld.

19 November 1991; accepted 20 February 1992

Metallo-Carbohedrenes: Formation of Multicage Structures

S. Wei, B. C. Guo, J. Purnell, S. Buzza, A. W. Castleman, Jr.*

An unusual structural growth pattern has been found in the system of Zr_mC_n, in which multicage structures are formed. The experimental evidence shows that the first cage closes at Zr_8C_{12}. Surprisingly, subsequent cluster growth does not lead to the enlargement of the cage size as it usually does in the case of pure carbon clusters and water clusters, for example. Rather, multicage structures are developed, that is, a double cage at $Zr_{13}C_{22}$ and $Zr_{14}C_{21/23}$, a triple cage at $Zr_{18}C_{29}$, and a quadruple cage at $Zr_{22}C_{35}$. This feature distinguishes the class of metallo-carbohedrenes from the regular doped fullerenes.

Recent studies have revealed the existence of a general class of materials, referred to as metallo-carbohedrenes, which have shown prominent species corresponding to the composition M_8C_{12}, M being Ti, V, Zr, and Hf (*1*, *2*). A cage-like pentagonal dodecahedron structure was proposed to account for their exceptional stability. We report further evidence supporting this cage-like structure, namely that cluster growth proceeds through the formation of multicage structures. Our new studies of clusters comprised of Zr_mC_n show that the first complete cage (Fig. 1A) closes at Zr_8C_{12}; subsequent attachment of metal-carbon units leads to the completion of double-cage structures (Fig. 1B) formed at $Zr_{13}C_{22}$ and $Zr_{14}C_{21/23}$, whereas a triple cage (Fig. 1C) is developed at $Zr_{18}C_{29}$ and a quadruple cage at $Zr_{22}C_{35}$ (Fig. 1D).

The apparatus used in these experiments is a reflectron time-of-flight (TOF) mass spectrometer coupled with a laser vaporization source. Metal-carbon clusters are produced through plasma reactions between metals and various small hydrocarbons (*1*, *3*), and the neutral clusters formed into a molecular beam are then ionized by an

Department of Chemistry, The Pennsylvania State University, University Park, PA 16802.

*To whom correspondence should be addressed.

Nd:YAG laser. The photoions are accelerated in the TOF lens region and detected by a microchannel plate detector. A typical TOF mass spectrum obtained through photoionization of Zr_mC_n at 532 nm is shown in Fig. 2; Zr_8C_{12} [the (8,12) peak] is the most abundant peak in the spectrum.

A careful examination of the mass spectrum reveals the presence of four distinct intensity groups, each of which displays truncation of intensity levels. One group encompasses the peaks corresponding to (8,12) and includes the three preceding peaks [the second peak labeled (a) being (6,10)]. An abrupt intensity drop after (8,12) gives rise to a second group comprised of six peaks [(9,16), (10,17), (11,19), (12,20), (13,22), and (14,23)]. The third group contains (15,25), (16,26), (17,28), and (18,29), and the fourth (19,31), (20,32), (21,34), and (22,35). Reproducible truncation occurs at (8,12), (14,23), (18,29), and (22,35). The truncations are indicative of structures of special stability and are consistent with cage closings leading to multicage structures as discussed below. Extensive investigations show that these features do not change under different experimental conditions, for example, over a range of ionization laser powers (from 10^7 to 10^{11} W/cm^2), at different laser wavelengths (266, 355, 532, and 1064 nm), and with a variety of hydrocarbons as reactant gas (CH_4, C_2H_2, C_2H_4, C_2H_6, and C_3H_6). The enhanced intensities of peak (a) (6,10) and peak (b) (10,17) are not always the same under different experimental conditions. In fact, in TOF-reflectron studies we find they exhibit appreciable metastable decay, showing that they are not magic numbers or stable species. Changes in their relative intensities can be accounted for in terms of the formation processes that will be discussed elsewhere (*3*).

The intensity anomalies (magic numbers) seen in the mass spectrum of clusters reflect their stabilities (*4*). Magic numbers do not always become manifested as prominent peaks, but more typically as a discontinuity, that is, a sudden intensity truncation in an otherwise smoothly varying distribution, which is indicative of the formation of clusters of unusual stability (such as

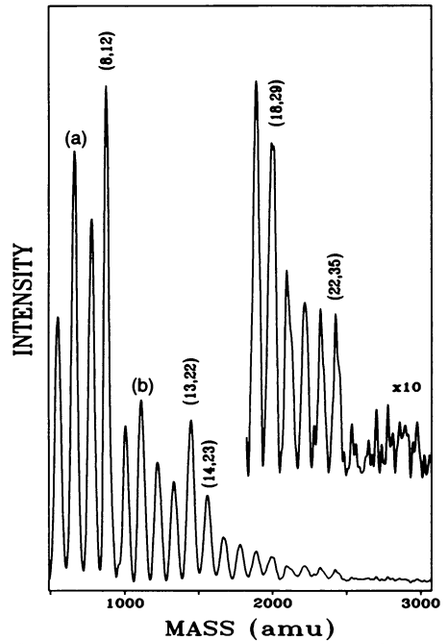

Fig. 2. A typical mass spectrum of Zr_mC_n. For simplicity of presentation, only the magic numbers are labeled as (*m,n*). The peaks labeled (a) and (b) are (6,10) and (10,17), respectively. These two peaks are not magic numbers as discussed in the text. The magic number at (8,12) marks the closure of the first cage-like structure, (13,22) and (14,23) indicate formation of a double-cage structure, whereas (18,29) and (22,35) reveal the closure of triple-cage and quadruple-cage structures. Other minor features can also be explained on the basis of partial closing of the cage (*3*).

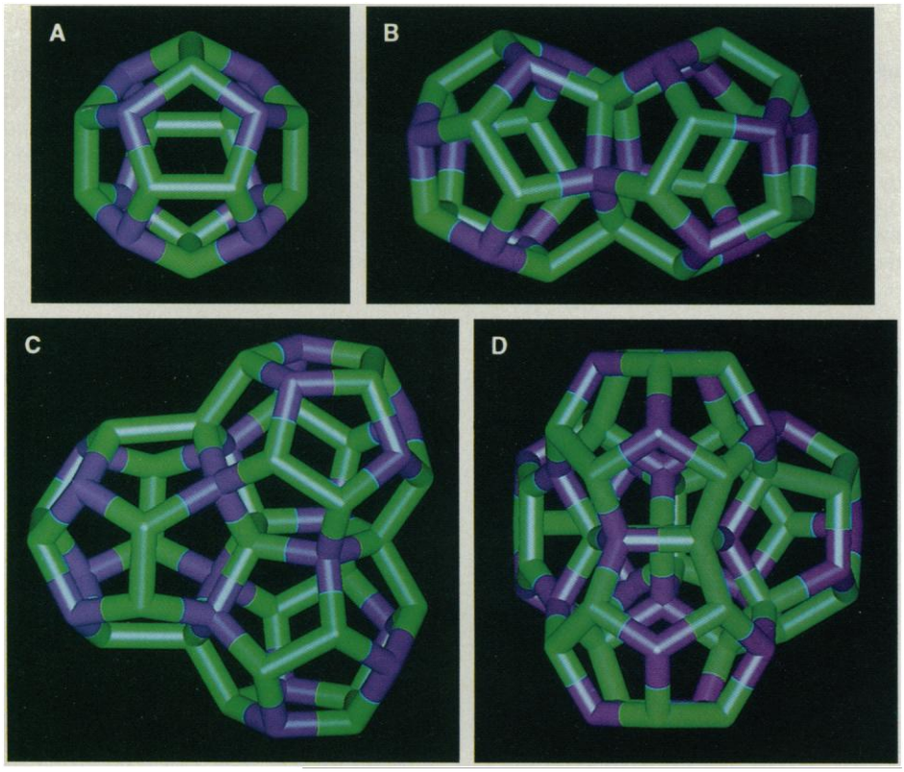

Fig. 1. (**A**) A proposed cage-like pentagonal dodecahedron structure of M_8C_{12}. The metal atoms are represented in purple and the carbon atoms are represented in green. (**B**) A proposed double-cage structure of $M_{14}C_{21}$. Note that when one of the 14 metal sites (purple) is occupied by one carbon atom, that is $M_{13}C_{22}$, the structure is also very stable. Two additional carbon atoms can form a pentagon through bridging between metal sites on two balls, leading to $M_{14}C_{23}$. (**C**) A proposed triple-cage structure of $M_{18}C_{29}$. (**D**) A proposed quadruple-cage structure. Note that other arrangements of the metal and carbon atoms are possible and that the structures are idealized, that is, no attempt is made to represent the sizes of the atoms or the bond lengths. However, the weaker metal-metal compared to metal-carbon–bonded arrangements are excluded.

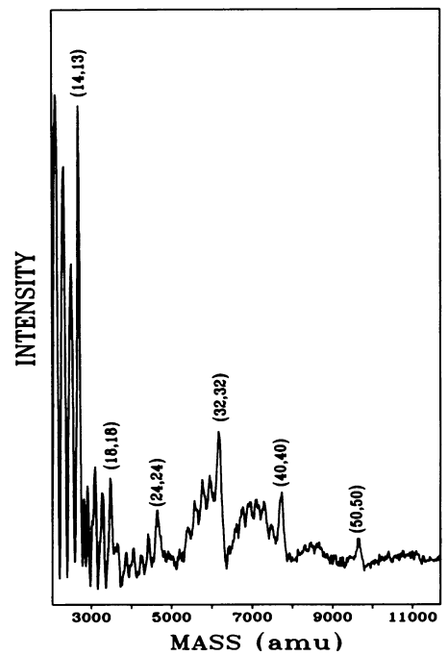

Fig. 3. A typical mass spectrum of Ta_mC_n. Magic numbers at (14,13), (18,18), (24,24), (32,32), (40,40), and (50,50) are indicative of cubic structures with close packing of 3 × 3 × 3, 3 × 3 × 4, 3 × 4 × 4, 4 × 4 × 4, 4 × 4 × 5, and 4 × 5 × 5, respectively.

closed-shell structures). In the present case, the magic number (8,12) observed in Fig. 2 is consistent with the closing of a cage-like pentagonal dodecahedron structure (Fig. 1A) (*1*). As for the subsequent growth of larger cluster sizes, there are two possibilities whereby the structure can rearrange to accommodate more atoms: (i) the breaking of pentagon rings and the formation of hexagon rings, as in the case of pure carbon clusters and water clusters, for example, and (ii) the addition of extra metal-carbon atoms to the basic unit, with the subsequent formation of multicage structures. In the case of pure carbon clusters, it is well known that an exceptionally stable cage exists with a total of 60 carbons, with other stable clusters involving different combinations of pentagons and hexagons (*5*). Likewise, for the system of water clusters, a pentagonal dodecahedron structure forms with 20 water molecules, whereas larger ones (such as 24 water molecules form a cage that consists of 2 hexagons and 12 pentagons) account for the observed magic number patterns (*6*). These structures cannot explain any of the magic numbers observed in the large cluster sizes of Zr_mC_n. However, multicage structures (discussed below) can account for all of our observations.

A completed double-cage structure is shown in Fig. 1B. A minimum of 35 atoms is required to construct the double cage, in accordance with the magic number at (13,22). For this combination, one of the possible metal positions, in Fig. 1B, is occupied by a carbon atom. In order to explain the magic number at (13,22) and the truncation at (14,23), the formation mechanism must be considered. As discussed in our earlier reports (*1*, *2*), the (8,12) species is very stable due to its lack of reactivity or growth, but the (8,13) and (8,14) species do exist and correspond to species with carbons on the periphery of the cage. These are identified as the origin of the multicage structures; growth by (1,2) and (2,3) additions (*3*) leads to formation of the (13,22) peak. Direct additions of (2,3) units lead to the (14,23) peak. The latter is a completed double-case structure having two additional carbons bridging between two metal sites, thereby closing another pentagon. Preliminary metastable studies reveal that these two carbons are relatively weakly bonded and are not members of the complete double cage (14,21) shown in Fig. 1B. Closed triple-cage (Fig. 1C) and quadruple-cage structures (Fig. 1D) require a minimum number of atoms corresponding to 47 and 57, respectively, in agreement with the experimental findings that magic numbers at (18,29) and (22,35) are observed in the mass spectrum.

It is instructive to compare and contrast these findings with another metal-carbon system that builds through the formation of cubic clusters. A typical TOF mass spectrum of Ta_mC_n clusters is shown in Fig. 3. A completely different magic number pattern exists for this system. All of the magic numbers at (14,13), (18,18), (24,24), (32,32), (40,40), and (50,50) are consistent with cubic structures (*7*) that have closed packings of $3 \times 3 \times 3$, $3 \times 3 \times 4$, $3 \times 4 \times 4$, $4 \times 4 \times 4$, $4 \times 4 \times 5$, and $4 \times 5 \times 5$. The failure to observe similar patterns in clusters Zr_mC_n implies that the cubic structures do not exist in this system, but rather, the cage-like structures are responsible for the magic numbers of metallo-carbohedrenes. Hence, while it might be suggested that a cubic structure with 8 metals at the corners and 12 carbons connecting in between could also explain the magic peaks we find at (8,12), such an explanation is not compatible with the growth mechanism of the metallo-carbohedrenes, nor could it account for the very definitive pattern seen for the development of multicage structures. This growth mechanism distinguishes the metallo-carbohedrenes as an unusual class of cluster materials.

REFERENCES AND NOTES

1. B. C. Guo, K. P. Kerns, A. W. Castleman, Jr., *Science* **255**, 1411 (1992).
2. B. C. Guo, S. Wei, J. Purnell, S. Buzza, A. W. Castleman, Jr., *ibid.* **256**, 515 (1992).
3. _____, manuscript in preparation.
4. T. P. Martin, T. Bergmann, H. Gohlich, T. Lange, *J. Phys. Chem.* **95**, 6421 (1991).
5. H. W. Kroto, A. W. Allaf, S. P. Balm, *Chem. Rev.* **91**, 1213 (1991).
6. S. Wei, Z. Shi, A. W. Castleman, Jr., *J. Chem. Phys.* **94**, 3268 (1991); A. Selinger and A. W. Castleman, Jr., *ibid.* **95**, 8442 (1991).
7. A. F. Well, Ed., *Structural Inorganic Chemistry* (Clarendon, Oxford, 1984).

8 Financial support by the U.S. Department of Energy, grant DE-FG02-ER-60668, is gratefully acknowledged. We thank Z. Shi, Z. Chen, B. May, S. Cartier, Y. Yamada, J. Ford, and E. Mereand for helpful discussions during the course of the work.

30 March 1992; accepted 13 April 1992

UV Spectrum and Proposed Role of Diethylberyllium in a ^{7}Li-^{7}Be Solar Neutrino Experiment

P. Dyer

Although measurement of the solar neutrino flux via the $^7Li(\nu_e,e^-)^7Be$ reaction was proposed many years ago, no experiment has been implemented since it has been difficult to identify a sensitive ^{7}Be detection technique. Here it is proposed that the ^{7}Be atom be incorporated into a volatile molecule, placed in a buffer-gas–filled cell, and then extracted by photodissociation; after excitation by a tunable laser, bursts of photons would be detected. The absorption spectrum of the molecular candidate diethylberyllium has been measured between 186 and 270 nanometers in a spectrophotometer to determine the required photodissociation laser wavelength and intensity.

The solution to the long-standing discrepancy between the calculated flux of the standard solar model and the smaller measured fluxes of the chlorine detector in the Homestake mine (*1*) and of the Kamiokande II water Čerenkov detector (*2*) may lie in the solar model or may have its roots in new neutrino physics. With results from the Soviet-American gallium experiment becoming available (*3*), there is increasing speculation that new physics may be required. As the neutrino spectrum would be different depending on whether solar model corrections or new physics is required, it is necessary to perform a number of complementary measurements with detectors having a range of energy thresholds.

A proposed measurement of the solar neutrino flux with a ^{7}Li detector, via the $^7Li(\nu_e,e^-)^7Be$ reaction, has been discussed for over 25 years (*4*, *5*). Lithium is a first-rate detector choice: it is cheap, the rate of neutrino events per ton is high, the neutrino energy threshold (862 keV) is relatively low, and the neutrino absorption cross sections can be calculated accurately. Techniques for extracting the ^{7}Be atoms from the lithium target have been developed, and a 1/100 scale model, with 2000 liters of 12 M lithium chloride, has been tested at Brookhaven National Laboratory, showing that it is possible to extract 100 μg of natural beryllium efficiently (*6*). Sources of background from α particles, neutrons, and cosmic rays were also studied. An experiment using metallic lithium is under development (*7*).

What has been lacking thus far is a means for efficiently detecting the few ^{7}Be atoms that would be produced by solar neutrinos. This nucleus has a half-life of 53 days and would be extremely hard to detect in small quantities by nuclear decay. The ^{7}Be nucleus decays 90% of the time to the ground state of ^{7}Li, producing Auger electrons with energy of only 50 eV, and only 10% of the time to

Physics Division, Los Alamos National Laboratory, Los Alamos, NM 87545.